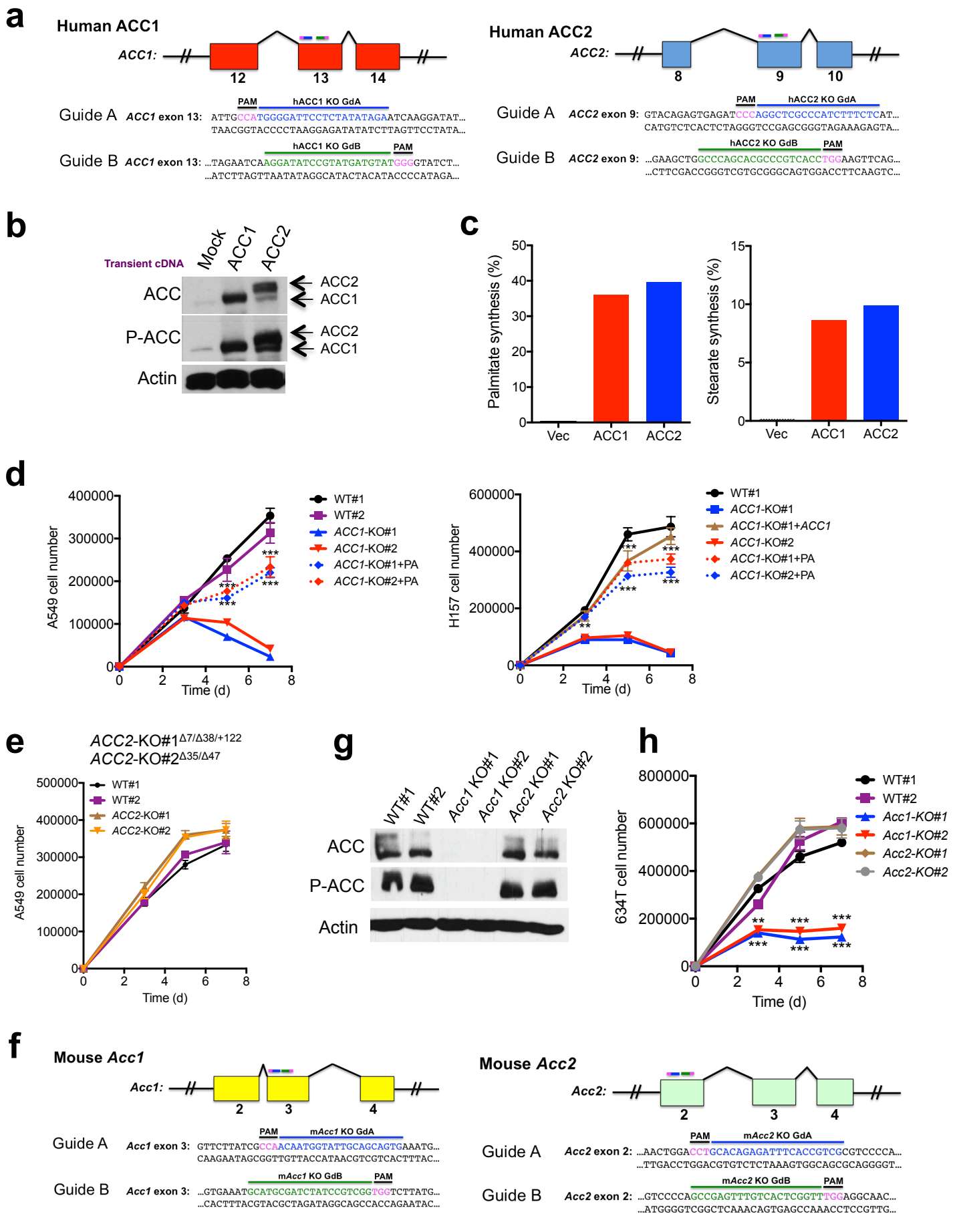

Supplemental Fig 1

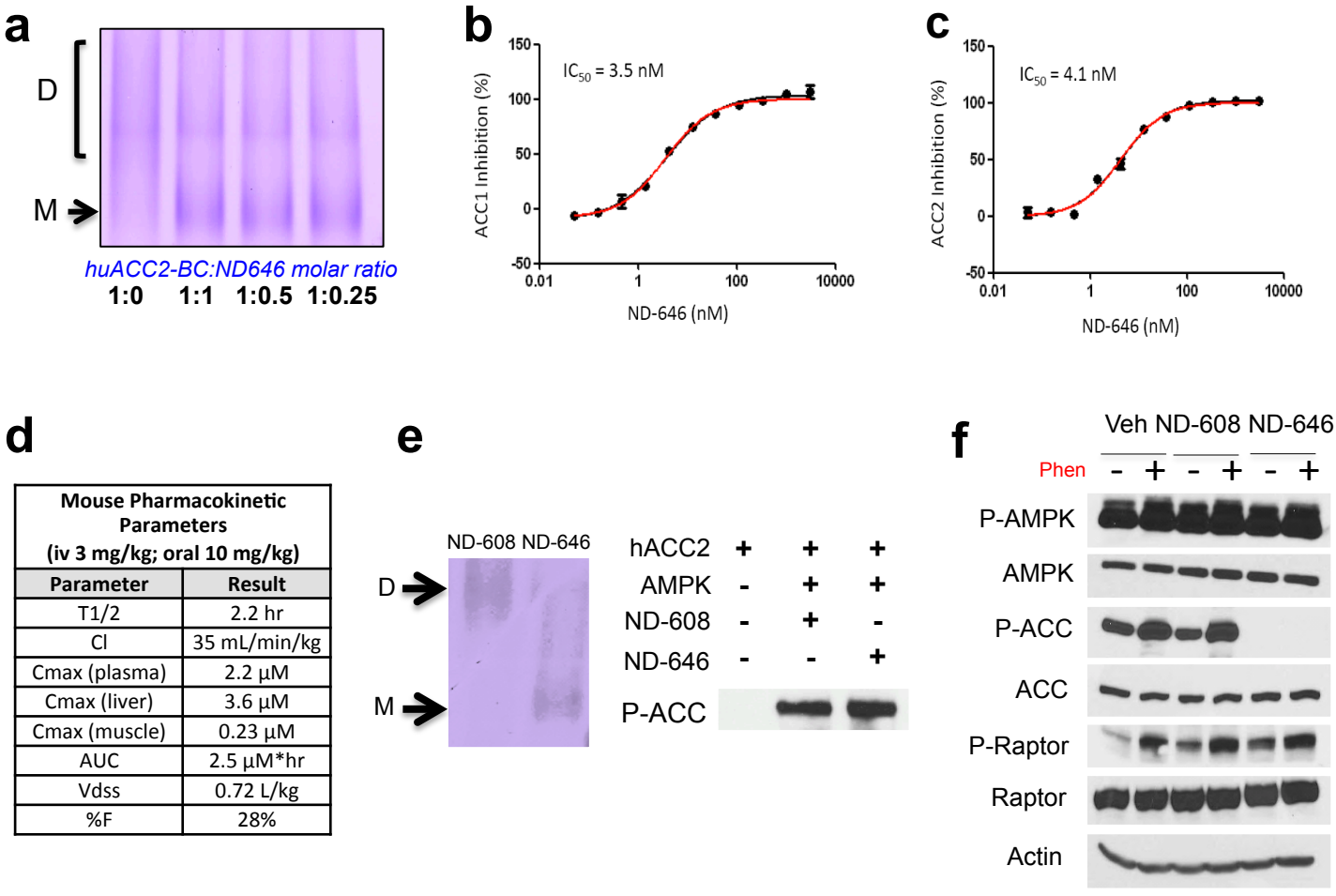

Mouse Pharmacokinetic Parameters (iv 3 mg/kg; oral 10 mg/kg)

Parameter	Result
T1/2	2.2 hr
Cl	35 mL/min/kg
Cmax (plasma)	2.2 µM
Cmax (liver)	3.6 µM
Cmax (muscle)	0.23 µM
AUC	2.5 µM*hr
Vdss	0.72 L/kg
%F	28%

ND-646 Tissue Exposure in A549 Mouse Tumor Model after 25 mg/kg oral dose

tumor inject. route	Plasma 1hr	Plasma 8hr	Tumor tissue 1hr	Tumor tissue 8hr	Lung tissue 1hr	Lung tissue 8hr
SubQ	23 µM (+/-3)	0.2µM (+/-0.2)	15 µM (+/- 11)	0.9 µM (+/-0.7)	21 µM (+/-17)	0.2 µM (+/-0.1)

Supplemental Fig 2

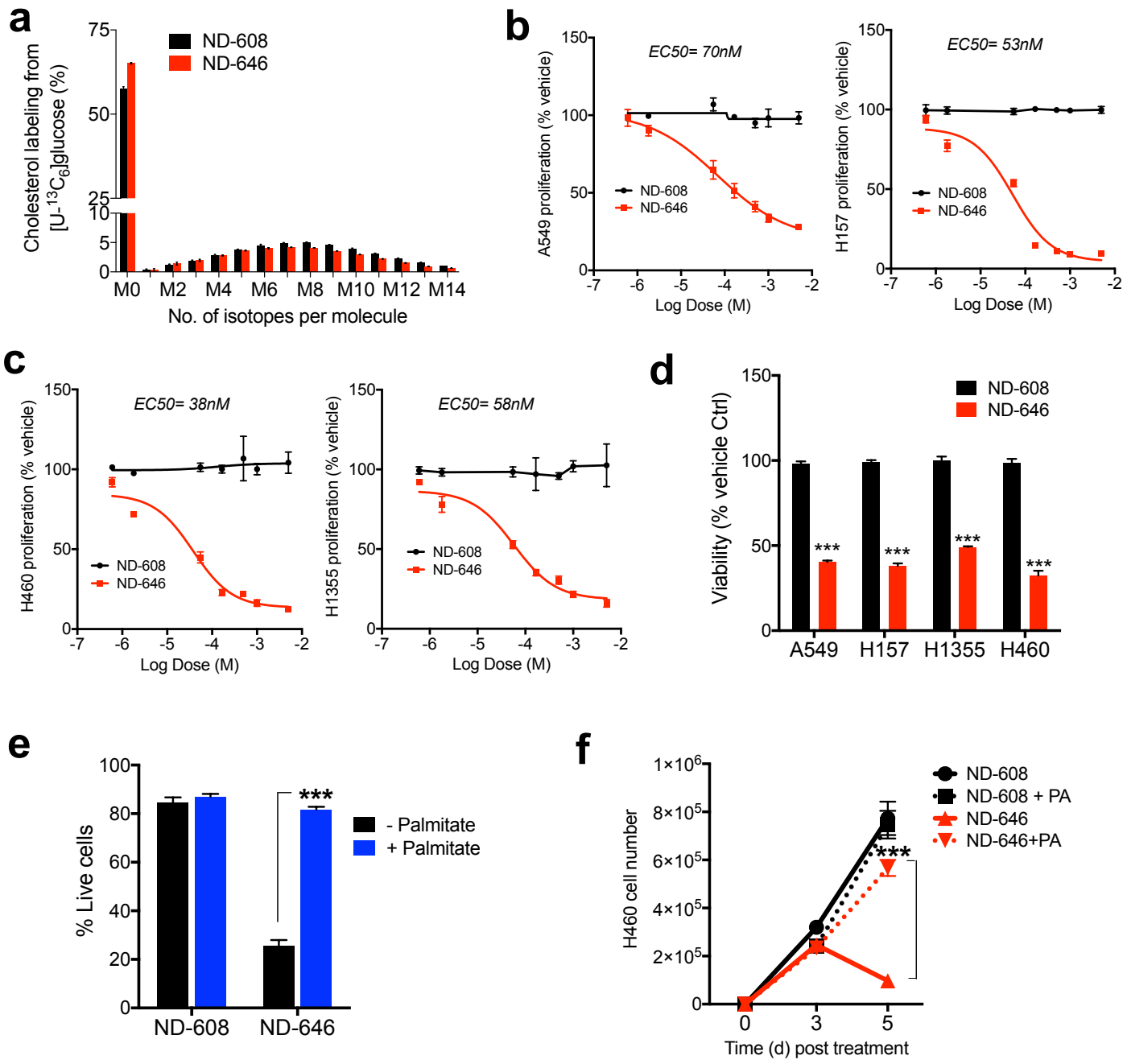

Supplemental Fig 3

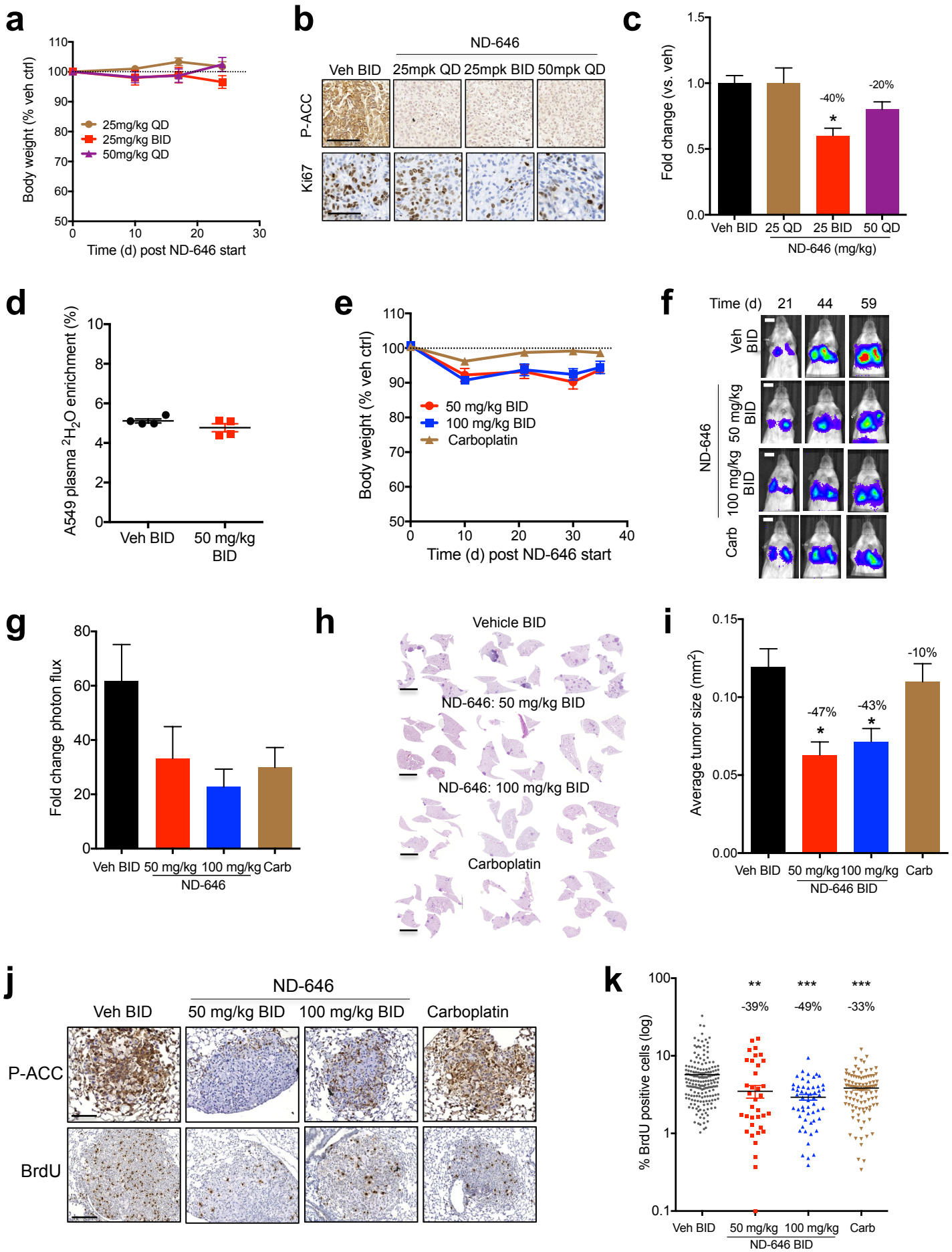

Supplemental Fig 4

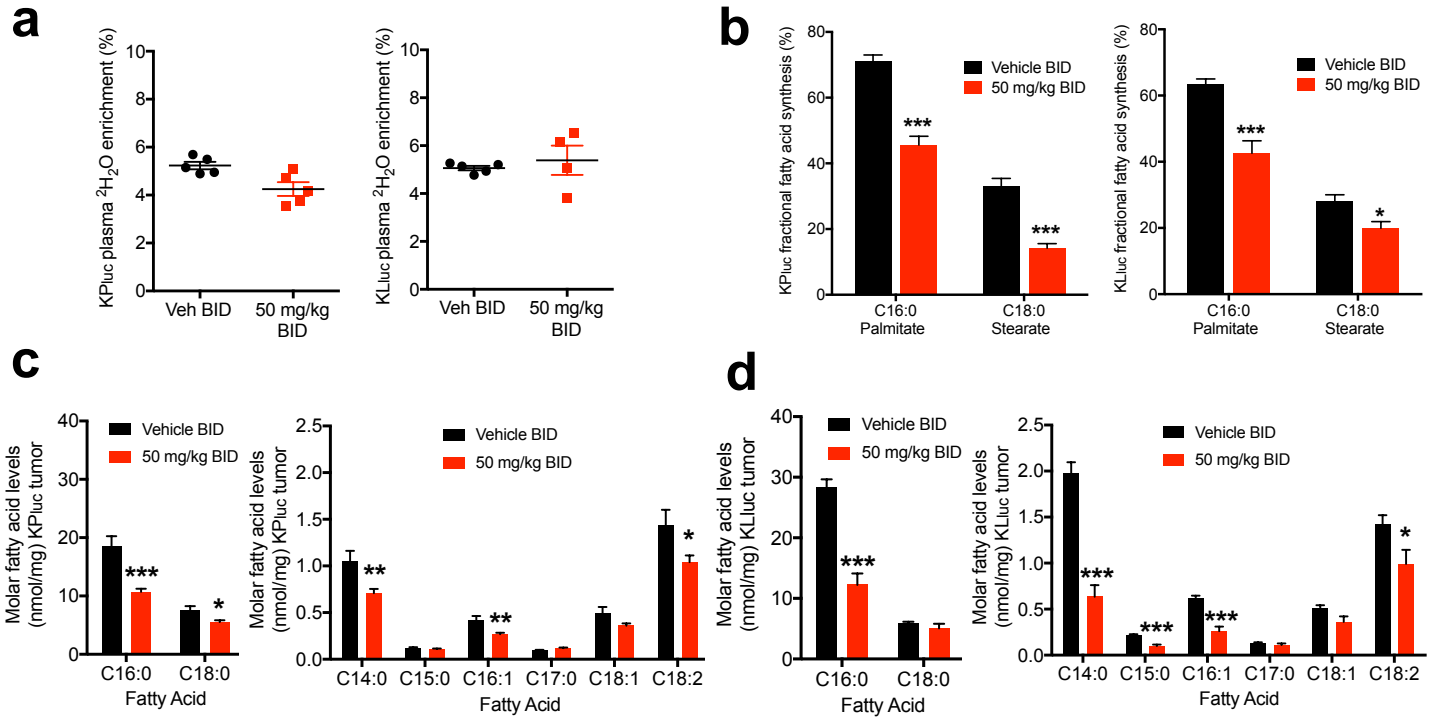

e

KP_{luc} Tumor FFAs (pmol/mg): 50 mg/kg BID vs. Vehicle					
FFA	Veh	ND-646	Sig?	P value	% Reduction
C16:2	1.30	1.39		0.811	-7.346
C16:1	54.11	33.78		0.146	37.583
C16:0	246.82	142.45	#	0.066	42.286
C18:3	16.35	6.12	#	0.063	62.569
C18:2	213.89	97.53	#	0.066	54.400
C18:1	207.60	109.17	#	0.099	47.412
C18:0	118.84	78.63	*	0.036	33.840
C20:5	8.03	4.26		0.147	46.909
C20:4	57.23	41.52		0.318	27.449
C20:3	7.73	4.86	#	0.096	37.073
C20:0	1.72	1.14		0.110	34.162
C22:6	42.80	32.18		0.322	24.810
C22:5	10.26	5.61	*	0.022	45.344
C22:1	0.56	0.69		0.410	-22.320
C22:0	0.65	0.44	*	0.034	33.013

KL_{luc} Tumor FFAs (pmol/mg): 50 mg/kg BID vs. Vehicle					
FFA	Veh	ND-646	Sig?	P value	% Reduction
C16:2	3.92	1.86	**	0.001	52.460
C16:1	84.54	40.81	**	0.003	51.722
C16:0	312.20	166.5	**	0.001	46.656
C18:3	17.47	15.2		0.540	12.713
C18:2	259.47	172.7	*	0.049	33.432
C18:1	295.56	179.3	*	0.013	39.335
C18:0	136.51	102.9	*	0.024	24.588
C20:5	9.62	3.5	*	0.035	63.853
C20:4	105.60	35.5	**	0.001	66.362
C20:3	12.57	8.7		0.132	30.835
C20:0	1.90	2.1		0.716	-7.885
C22:6	88.10	37.5	**	0.008	57.483
C22:5	14.47	9.9		0.148	31.840
C22:1	1.53	1.3		0.492	17.148
C22:0	0.86	0.7		0.131	24.518

f

KP_{luc} Plasma FFAs (μM): 50 mg/kg BID vs. Vehicle					
FFA	Veh	ND-646	Sig?	P value	% Reduction
C16:2	1.69	1.04	#	0.0538	38.378
C16:1	39.77	22.77	*	0.0216	42.754
C16:0	139.68	80.52	*	0.0250	42.355
C18:3	27.50	13.99	*	0.0154	49.131
C18:2	197.77	125.67	*	0.0362	36.457
C18:1	152.21	108.03		0.1616	29.023
C18:0	51.04	28.30	**	0.0052	44.548
C20:5	8.42	1.73	*	0.0138	79.502
C20:4	23.99	9.75	*	0.0218	59.372
C20:3	3.66	2.07		0.1726	43.511
C20:0	0.72	0.67		0.6926	6.692
C22:6	42.12	17.91	*	0.0327	57.474
C22:5	4.26	1.33	*	0.0296	68.676
C22:1	0.22	0.25		0.4034	-16.245
C22:0	0.24	0.19		0.3909	21.124

KL_{luc} Plasma FFAs (μM): 50 mg/kg BID vs. Vehicle					
FFA	Veh	ND-646	Sig?	P value	% Reduction
C16:2	1.72	0.91	*	0.0272	47.469
C16:1	29.99	20.08		0.2270	33.041
C16:0	120.62	63.90	*	0.0272	47.026
C18:3	17.89	11.63		0.1469	34.997
C18:2	147.06	97.33	*	0.0337	33.816
C18:1	129.00	80.20	*	0.0381	37.830
C18:0	39.36	24.33	**	0.0042	38.200
C20:5	2.18	2.08		0.8920	4.329
C20:4	17.72	6.80	*	0.0199	61.599
C20:3	2.06	1.52		0.1558	26.034
C20:0	0.48	0.69		0.1147	-43.137
C22:6	18.26	15.62		0.3530	14.458
C22:5	1.54	1.52		0.9543	1.521
C22:1	0.19	0.27		0.1412	-43.375
C22:0	0.10	0.16		0.1709	-71.079

Supplemental Fig 5

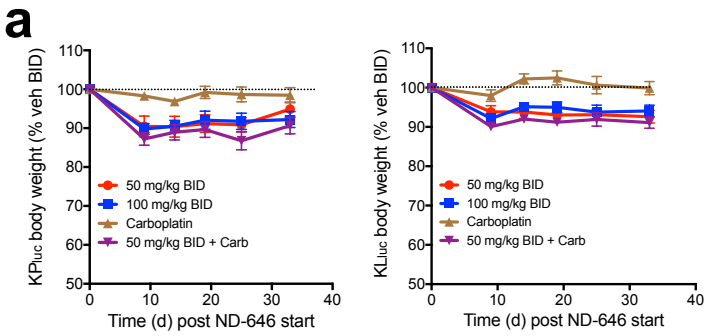

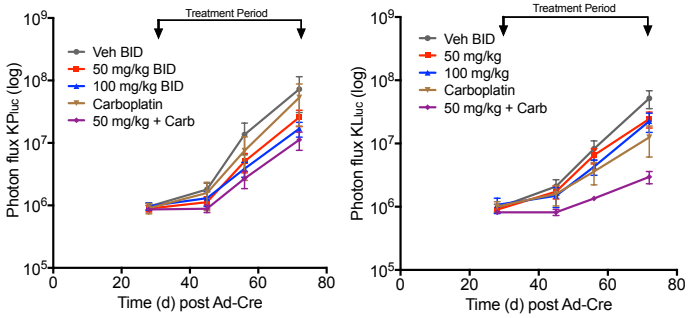

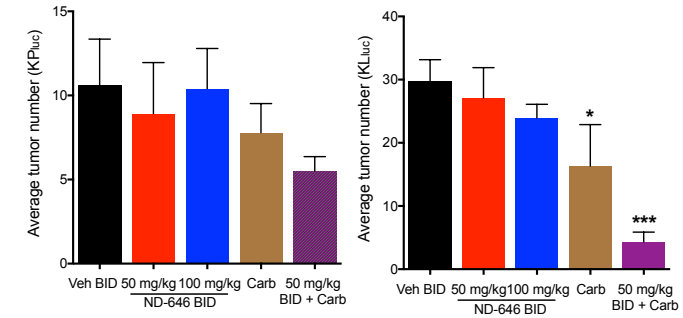

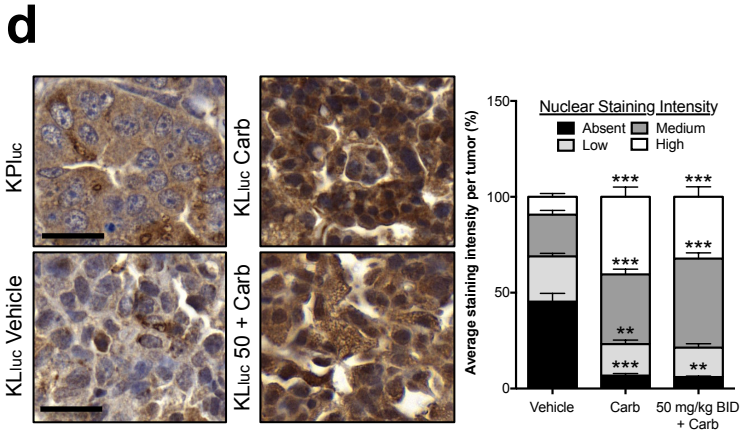

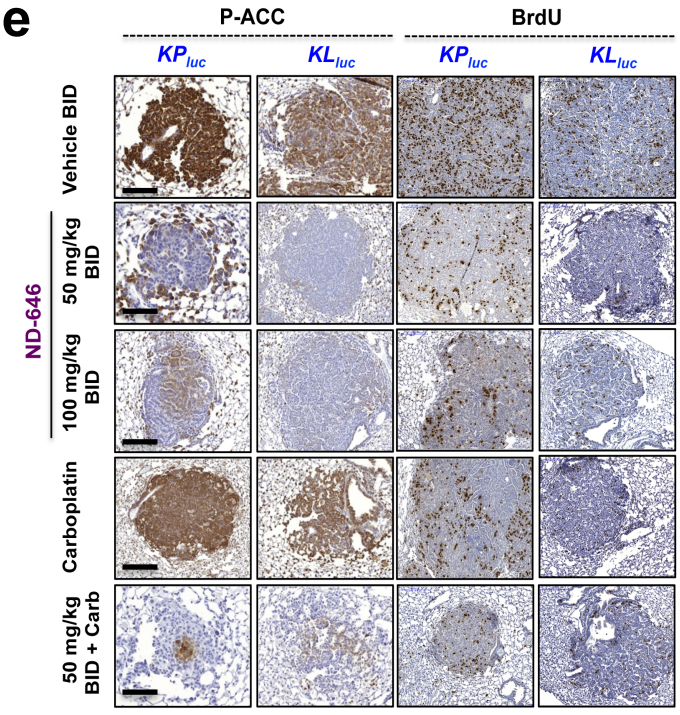

f

50 mg/kg BID vs. Vehicle			
FFA	Sig?	P-value	% Reduction
C16:2	*	0.0382151	82.00
C16:1		0.0765149	59.28
C16:0		0.0683066	39.97
C18:3		0.0926874	93.59
C18:2	*	0.0370077	81.21
C18:1		0.174106	43.41
C18:0		0.371298	11.16
C20:4		0.0780851	90.35
C20:3	*	0.046039	86.88
C20:0		0.372981	12.02
C22:1		0.998532	-0.11
C22:0		0.341628	16.32

100 mg/kg BID vs. Vehicle			
FFA	Sig?	P-value	% Reduction
C16:2	*	0.039728	83.77
C16:1		0.0959206	63.86
C16:0		0.0612895	51.87
C18:3		0.097827	92.18
C18:2	*	0.0251493	92.61
C18:1		0.148722	56.36
C18:0		0.308039	16.84
C20:4		0.0619761	97.71
C20:3	*	0.0408024	91.18
C20:0		0.711665	-5.69
C22:1		0.976913	1.16
C22:0		0.667024	7.82

g

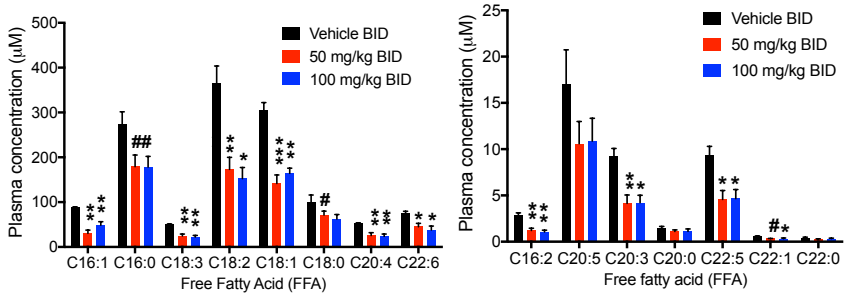

KPluc Plasma Free fatty Acids (μM): ND-646 vs. Vehicle									
FFA	Veh	50 mg/kg	% Reduction	Sig?	P-value	100 mg/kg	% Reduction	Sig?	P-value
C16:2	2.92	1.06	63.69	**	0.0011	1.22	58.18	**	0.0050
C16:1	87.57	48.63	44.47	**	0.0092	30.44	65.24	**	0.0016
C16:0	272.69	178.09	34.69		0.0516	179.09	34.32		0.0735
C18:3	49.64	22.14	55.40	**	0.0022	24.66	50.31	**	0.0053
C18:2	365.54	152.62	58.25	**	0.0044	173.19	52.62	*	0.0145
C18:1	304.35	164.15	46.07	***	0.0010	141.63	53.47	**	0.0034
C18:0	100.43	62.28	37.99		0.0828	71.14	29.17		0.1757
C20:5	17.06	10.88	36.24		0.2049	10.59	37.95		0.2153
C20:4	52.47	23.83	54.59	**	0.0052	25.63	51.15	*	0.0145
C20:3	9.22	4.21	54.32	**	0.0085	4.15	54.99	*	0.0152
C20:0	1.52	1.13	25.74		0.2712	1.12	26.43		0.1205
C22:6	74.51	37.85	49.20	*	0.0219	45.14	39.42	*	0.0334
C22:5	9.31	4.66	49.95	*	0.0224	4.57	50.95	*	0.0265
C22:1	0.56	0.32	42.59		0.0940	0.33	40.62	*	0.0362
C22:0	0.43	0.32	24.68		0.3591	0.29	31.31		0.1542

Supplemental Fig 6

SUPPLEMENTAL FIGURE LEGENDS

Supplemental Figure 1. ACC1 is required for growth and viability of non-small cell lung cancer cells *in vitro* and *in vivo*. (**a**) Schematic of gRNA design targeting human *ACC1* or *ACC2*. (**b**) Western blot for ACC and P-ACC in wild-type HEK293T cells transiently expressing either mock, full length *ACC1* or *ACC2*. (**c**) Palmitate (left) and stearate (right) synthesis in a [U-$^{13}C_6$]glucose labeled HEK293T *ACC1*-KO clone transiently expressing either empty vector, human *ACC1* or *ACC2* cDNA for 48hrs. (**d**) Cellular growth curves of A549 (left) and H157 (right) WT and *ACC1*-KO clones in delipidated FBS in the presence or absence of 200 μM exogenous palmitate (PA). Triplicate cell counts were taken at days 3, 5 and 7. (**e**) CRISPR/Cas9 deletion of *ACC2* in A549 cells and cellular growth curves of WT and *ACC2*-KO clones. Triplicate cell counts were taken at days 3, 5 and 7. Mutations in *ACC2* genomic DNA in clones are highlighted. (**f**) Schematic of gRNA design targeting mouse *Acc1* or *Acc2*. (**g**) Representative western blot of CRISPR/Cas9 deletion of *Acc1* or *Acc2* in 634T mouse NSCLC cells. (**h**) Cellular growth curves of WT, *Acc1* -KO and *Acc2*-KO 634T clones. Triplicate cell counts were taken at days 3, 5 and 7. All values are expressed as means ± s.e.m. * P<0.05 ** P<0.01 *** P<0.001 relative to WT determined using ANOVA with Tukeys method for multiple comparison (**d**, **h**).

Supplemental Figure 2. Properties of ND-646 *in vivo*. (**a**) Native electrophoresis mobility shift assay to assess dimerization of recombinant BC domain human ACC2 (hACC2-BC) in the absence or presence of ND-646 at the indicated mole:mole ratios. D = dimer, M= Monomer. (**b**) Inhibition of hACC1 enzymatic activity and (**c**) inhibition of hACC2 enzymatic activity as a function of ND-646 concentration in cell free assays. (**d**) Table of pharmacokinetic parameters determined after a single 3 mg/kg intravenous or 10 mg/kg oral dose of ND-646. (**e**) Left panel: Native electrophoresis mobility shift assay, **D** = dimer, **M** = monomer. Right panel: *in vitro* kinase assay followed by P-ACC western blot of hAAC2-BC domain bound to either ND-608 or ND-646 ± recombinant AMPK. (**f**) Analysis of the effects of 500 nM ND-646 on AMPK activation in A549.LKB1 cells after 2 mM phenformin treatment for 1hr. Cells were immunblotted for phosphorylation of AMPK substrates. (**g**) *in vitro*

AMPK kinase assay western blot analysis of recombinant wild-type (WT), arginine to alanine mutant (R277A) or serine to alanine mutant (S222A) hACC2-BC. (**h**) ND-646 tissue exposure in plasma, subcutaneous A549 tumors or normal lung tissue after 1 hr or 8 hr post single oral dose of ND-646 at 25 mg/kg. Values represent average (n=3) μM levels (± sem) of ND-646 quantitated in each tissue. (**i**) Pharmacodynamic analysis of ND-646 using the P-ACC biomarker in A549 tumors. Mice bearing subcutaneous A549 tumors were dosed orally with a single dose of ND-646 at 25 mg/kg and tumors were harvested 1 hr and 8 hr post dosing for assessment of P-ACC. Numbers correspond to individual tumors from separate mice (n=3 mice per treatment).

Supplemental Figure 3. ND-646 inhibits fatty acid synthesis *in vitro* and induces apoptosis and ER stress in NSCLC cells.

(**a**) Cholesterol mass isotopomer distribution (MID) in A549 cells labeled with [U-$^{13}C_6$]glucose. Cells were treated for 24 hrs with either 500 nM ND-608 or ND-646. (**b)** Cellular growth and EC_{50} analysis of human NSCLC cell lines A549 (left), H157 (right) and (**c**), H460 (left) and H1355 (right) treated with vehicle or a dose response (5000 nM, 1000 nM, 500 nM, 166 nM, 55 nM, 18 nM, 6 nM) of either ND-608 or ND-646. Triplicate cell counts were recorded and data is represented as percent growth (proliferation) at day 7-post treatment normalized to percent vehicle control. EC_{50} values are highlighted in each panel for each cell line. (**d**) Viability assay of A549, H157 and H460 cells treated with vehicle, 500 nM ND-608 or 500 nM ND-646 for 7 days. Data are represented as percent viability normalized to vehicle control. (**e**) Cell viability measured by trypan blue exclusion assay of A549 cells co-treated for 7 days with either 500 nM ND-608 or 500 nM ND-646 and 200 μM palmitate conjugated to BSA. (**f**) Cell growth analysis of H460 cells co-treated with either 500 nM ND-608 or 500 nM ND-646 and 200 μM palmitate (PA) conjugated to BSA. Triplicate cell counts were taken at days 3 and 5-post treatment. Data represented as average cell number ± s.e.m per treatment condition at each time point. (**g**) Western analysis of P-ACC status of ND-646 or ND-646 + palmitate (PA) treated A549 cells. Lysates were prepared after 3 days of treatment. (**h**) ER stress analysis in lysates of A549 cells treated with either 500 nM ND-608 or 500 nM ND-646 in media containing either regular FBS (Reg) or delipidated FBS (Del) at 3, 4 and 5 days post treatment. Cells were analyzed for expression of early markers (P-EIF2α^{S51}) and late markers (CHOP) of ER

stress and for P-ACC. All values are expressed as means ± s.e.m. * P<0.05 ** P<0.01 *** P<0.001 relative to ND-608 control determined using ANOVA with Tukeys method for multiple comparison (**d**, **e**, **f**).

Supplemental Figure 4. ND-646 inhibits FASyn and tumor growth in NSCLC xenograft models. (**a**) Body weights of mice bearing subcutaneous A549 tumors during chronic ND-646 dosing. Data are represented as percent change in body weight vs. vehicle. (**b**) IHC for P-ACC and Ki67 in A549 tumors. Images are representative examples from 5-6 regions of each tumor for each treatment condition. Scale bar =100 μm. (**c**) Quantitation of IHC staining for Ki67 in A549 tumors. (**d**) Deuterium enrichment in plasma H_2O of mice bearing A549 lung tumors treated with vehicle or ND-646. Each dot represents plasma from a single mouse. (**e**) Body weights of mice during chronic ND-646 dosing in mice bearing A549 lung tumors. Data are represented as percent change in body weight vs. vehicle. (**f**) Representative bioluminescence overlay images of ND-646 efficacy in the A549 lung tumors. Images are representative for each treatment condition. Scale bar =1 cm. (**g**) Fold change in bioluminescence (photon flux) for each treatment group during the treatment period (day 21 to day 63). (**h**) Representative H&E stained sections of A549 lung tumors for each treatment group. Scale bar = 5000 μm. (**i**) Average A549 lung tumor size (mm^2) for each treatment condition. (**j**) IHC for P-ACC and BrdU in A549 tumors. Images are representative examples for each treatment condition. Scale bar =100 μm. (**k**) BrdU positivity of tumors from each treatment condition (log scale). % of BrdU positive cells per tumor was quantified and each dot represents an individual tumor. For each graph, values are expressed as means ± s.e.m. * P<0.05 ** P<0.01 *** P<0.001 relative to WT control determined using two tailed students t test (**c**, **i**) or ANOVA (**k**) with Tukeys method for multiple comparison.

Supplemental Figure 5. ND-646 inhibits FASyn in lung tumors of $Kras^{G12D}$ $p53^{-/-}$ and $Kras^{G12D}$ $Lkb1^{-/-}$ mouse models of NSCLC and lowers plasma free fatty acids. (**a**) Deuterium enrichment in plasma H_2O of mice bearing KP_{luc} (left) or KL_{luc} (right) lung tumors treated with vehicle or ND-646. Each dot represents plasma from a single mouse. (**b**) Fractional *de novo* palmitate (C16:0) and stearate (C18:0) synthesis is shown in KP_{luc} lung

tumors (left) and KL^{luc} lung tumors (right) after 1 week of ND-646 treatment (PO). 3 tumors per mouse were analyzed (15 tumors total per treatment). (**c**) Molar levels of total fatty acids in KP^{luc} and (**d**) KL^{luc} lung tumors treated with either vehicle or ND-646. Left graph depicts high abundance fatty acids; right graph depicts low abundance fatty acids. (**e**) Table showing percent reduction of free fatty acids (FFA) in lung tumors from KP^{luc} (left) and KL^{luc} (right) mice treated with vehicle or ND-646. Table shows FFA, average level (pmol/mg tumor) in Vehicle or ND-646 treated mice, significance, p-value and percent reduction (vs. vehicle). Orange rows depict p-values >0.05 and < 1. (**f**) Table showing percent reduction of free fatty acids (FFA) in plasma of KP^{luc} (left) and KL^{luc} (right) mice treated with vehicle or ND-646. Table shows FFA, average level (μM) in Vehicle or ND-646 treated mice, significance, p-value and percent reduction (vs. vehicle). For each graph and table, values are expressed as means ± s.e.m. # = 0.05< p <0.1 * P<0.05 ** P<0.01 *** P<0.001 relative to vehicle treatment determined by two sided students t test.

Supplemental Figure 6. ND-646 inhibits tumor growth in Kras^{G12D} p53$^{-/-}$ and Kras^{G12D} Lkb1$^{-/-}$ autochthonous NSCLC models. (**a**) Body weights of mice during chronic ND-646 dosing in KP^{luc} (left) and KL^{luc} (right) mice. Data are represented as percent change in body weight vs. vehicle. (**b**) Growth of KP^{luc} (left) and KL^{luc} (right) lung tumors treated with vehicle BID, ND-646 50 mg/kg BID, or 100 mg/kg BID, Carboplatin 25mg/kg every 3 days or ND-646 50 mg/kg BID + Carboplatin. Data are represented as average bioluminescence (photon flux log scale) per treatment group vs. days post Ad-cre inhalation. Treatment period is highlighted on top of graph. (**c**) Average tumor cell number in KP^{luc} (left) and KL^{luc} (right) mice per treatment condition. (**d**) IHC for p53 in KL^{luc} lung tumors treated with carboplatin or ND-646 50 mg/kg BID + carboplatin. KP^{luc} IHC demonstrates specificity of the p53 nuclear stain. Right graph shows quantitation of nuclear stain intensity, using inForm analysis. Scale bar = 20 μm (**e**) IHC for P-ACC and BrdU in KP^{luc} and KL^{luc} lung tumors. Images are representative examples for each treatment condition. Scale bar = 100 μm (**f**) Table showing quantitation of free fatty acids in livers of KP^{luc} mice treated with either vehicle or ND-646. Orange rows depict p-values >0.05 and < 1. (**g**) Quantitation of individual free fatty acids (FFA) in plasma from KP^{luc} mice treated with either vehicle or

ND-646. Left panel shows high abundance FFAs and right panel shows low abundance FFAs. Table shows FFA, average level (μM) in Vehicle or ND-646 treated mice, significance, p-value and percent reduction (vs. vehicle). For each graph and table data are expressed as means ± s.e.m. # = 0.05< p <0.1 * P<0.05 ** P<0.01 *** P<0.001 relative to vehicle treatment determined by two sided students t test.

SUPPLEMENTAL METHODS

ACC1 and ACC2 inhibition. Cell free ACC inhibition was assessed using a luminescent ADP detection assay (ADP-Glo™ Kinase Assay Kit; Promega) as described in Harriman et al[19], using either recombinant hACC1 (BPS Biosciences Catalog #50200) or recombinant hACC2 (BPS Biosciences Catalog #50201) as the source of enzyme.

Antibodies and reagents. Antibodies from Cell Signaling Technologies (Denvers, MA USA) were diluted 1:1000 and included P-ACC^{S79} (#3661), P-AMPK^{T172} (#2535), P-Raptor (#2083), P-EIF2α^{S51} (#3597), CHOP (#5554), ACC (#3662), AMPKα (#2532), LKB1 (#3047), PARP (#9532), GST (#2622), Raptor (#2280), cleaved Caspase 3 (#9661). Anti-BrdU (Abcam #6326) and p53 (clone CM5) were used for IHC. Anti-actin antibody (#A5441) diluted 1:10000 was purchased from Sigma-Aldrich. Antibody validation is provided on the manufacturers website for each antibody used. For Calyculin-A (Millipore #19-139) treatment, cells in a monolayer were treated with 30 mM of Calyculin-A for 30 mins prior to lysis and western analysis by SDS-PAGE.

Lipid Extraction. Lipid extraction was performed as described[43,44]. Briefly, tumors (20 mg) were Dounce homogenized on ice in a mixture of 1 mL PBS, 1 mL MeOH, and 2 mL $CHCl_3$. For plasma, 100 µL of plasma was added to 1.4 mL PBS, followed by the addition of 1.5 mL MeOH and 3 mL $CHCl_3$. 200 pmol of $^{13}C_{16}$-palmitic acid was added to the chloroform as an internal standard prior to extraction. Mixtures were vortexed and then centrifuged at 2200 g for 5 min to separate the aqueous and organic layer. The organic phase containing the extracted lipids was collected and dried under N_2 and stored at -80 °C before LC-MS analysis.

Fatty acid profiling and Isotopomer Spectral Analysis (ISA). For fatty acid profiling experiments, 1 μg of deuterated ($^2H_3$) standards (C14:0, C15:0, C16:0, C17:0, C18:0) were added during extraction. The ratio of deuterated (M+3) to unlabeled (M+0) fatty acids was used for molar quantification. A model for palmitate biosynthesis, whereby eight acetyl-CoA molecules are consumed to form one palmitate molecule, was generated to estimate the rate of de novo synthesis from experimental palmitate mass isotopomer distributions. Parameters for the relative enrichment of lipogenic acetyl-CoA from a given 13C tracer and the percentage of fatty acids that are de novo synthesized are extracted from a best-fit model using the INCA MFA software package [45]. The 95% confidence intervals for both parameters were estimated by sensitivity analysis of the sum of squared residuals between measured and simulated palmitate mass isotopomer distributions to small flux variations [46].

Expression and purification of recombinant hACC2-BC domain. Human ACC2 BC domain (residues 217-775) was cloned into a pGEX-2T plasmid (GE Healthcare #28-9546-53) containing an N-terminal GST-tag and affinity purified from *E.coli*. Purified protein was concentrated using an Amicon Ultra-15 centrifugal filter unit and protein concentration was measured using a Pierce BCA protein assay kit using a BSA standard. Protein purity was determined using coomasie stained SDS-PAGE.

Western blots and native PAGE. For biochemical analysis of tumors, tumors were immediately snap frozen in liquid nitrogen and homogenized on ice in lysis buffer. Lysates were equilibrated for protein levels using a BCA protein assay kit (Pierce) and resolved on 8% SDS-PAGE gels depending on the experiment. For biochemical analysis of cells, cell lysates were prepared in lysis buffer, centrifuged and equilibrated for protein levels as above. Lysates were resolved on 8-12% SDS-PAGE gels depending on the experiment. Original western blots can be found in the supplemental data set. For Native PAGE experiments, hACC2-BC was first subject to a dimerization assay in the presence or absence of increasing molar ratios of ND-646. Briefly, 100 μM of purified hACC2-BC was combined with ND-646 in a final volume of 20 μl and incubated at 4 °C for 1 hr. 6 μl of native sample buffer (Life Technologies #BN2003) and 1 μl of 5% G250 (Life Technologies #BN2004) were then added to the reaction and samples were loaded onto a 8% Bis-Tris native polyacrylamide gel. G250 was added to the

cathode buffer and samples were allowed to migrate for ~12hrs at 70V. The gel was washed overnight in water and images were subsequently taken.

Plasmids. A donor vector (pDONR221) containing full-length human ACC1 cDNA was created from a TOPO plasmid containing full-length human ACC1 (Dharmacon, #MHS6278-213245945) by PCR with primers containing the AttB sites. For ACC2, full-length human ACC2 cDNA was purchased in pENTR223.1 (DNASU, clone HsCD00353997). For wild type ACC expression studies, full-length cDNAs underwent a LR reaction into a plenti-DEST-Puro vector (Addgene #17452) by Gateway cloning using LR clonase II. $ACC1^{R172A}$ and $ACC2^{R277A}$ and $ACC2^{S222A}$ mutants were generated by site directed mutagenesis. For transient transfection studies, 1 μg of plasmid was transfected into HEK293T cells using lipofectamine 2000 according manufacturers conditions. HEK293T cells were transfected for 24hrs before being treated with either ND-646 or Calyculin A.

***In vitro* kinase assay.** 1 μg of recombinant wild-type or mutant hACC2-BC domain was added to 0.2 U of recombinant AMPK (Millipore #14-840) in a 30 μl solution containing 1 M MgCl2, 50 mM Tris pH 7.5 and 10 mM NaCl for 1 hr at 30 °C. 6 μl of sample buffer was then added and boiled for 5mins. The reaction product was then analyzed via SDS-PAGE for phosphorylation of ACC using the P-ACC antibody.

Protein crystallography and molecular modeling. Technical descriptions are available in Harriman et al[19]

SUPPLEMENTAL METHODS REFERENCES

43. Bligh, E.G. & Dyer, W.J. A rapid method of total lipid extraction and purification. *Can J Biochem Physiol* **37**, 911-917 (1959).
44. Saghatelian, A., *et al*. Assignment of endogenous substrates to enzymes by global metabolite profiling. *Biochemistry* **43**, 14332-14339 (2004).
45. Young, J.D. INCA: a computational platform for isotopically non-stationary metabolic flux analysis. *Bioinformatics* **30**, 1333-1335 (2014).
46. Antoniewicz, M.R., Kelleher, J.K. & Stephanopoulos, G. Determination of confidence intervals of metabolic fluxes estimated from stable isotope measurements. *Metabolic engineering* **8**, 324-337 (2006).